molecular shape emerged. The bulk modulus is a convenient index of packing efficiency.

(9) Molecular shape is roughly coded by ratios of moments of inertia. Aromatic, rigid, cylindric molecules pack in such a way that the elongation axes are very nearly parallel.

(10) A principal-component analysis reveals three moments, which can be interpreted as a size parameter, a packing tightness parameter, and a packing failure parameter. Compounds of similar molecular shapes are grouped in moments space.

The hydrocarbon files are susceptible to many future uses: molecule-to-molecule energies and the composition of the coordination shell, with the distribution of interatomic contacts, deserve further examination; the shape factor can be coded after the analysis of the differences between molecules of the same size but with different packing energies; the packing of isomers, or of the same molecule in different crystal phases, can be examined; molecular reorientations can be studied, and the barriers can be calculated and related to molecular shape; the performance of different potential energy parameters can be tested over a much larger basis than is normally used in their derivation. Even more important as a further step is, however, the study of the influence of substituents of moderate polarity (heteroatoms in cycles, chlorine versus methyl) on the packing standards we have outlined for hydrocarbon cores and even the analysis of how groups with larger dipole moments (cyano or carbonyl groups) may perturb the geometrical features of hydrocarbon packing.

Appendix

For the retrieval of crystal data from the Cambridge SD, classes[1b] 5 and 19–31 were considered, for substances containing only C and H atoms. Disordered structures, inclusion compounds, and solvates were excluded. When more than one determination was reported for the same compound, the most recent one, or the one nearest to room temperature, was retained. Thus, the overwhelming majority of data refer to room-temperature analyses. When more than one polymorph or optical isomer was available, all were included in the data set.

In a first step, years 1975–1986 were considered. No R factor threshold was imposed, since intermolecular properties are sensitive to the general packing pattern, and much less to details in the refinement of the structure. In a second step, the search ran over years 1930–1974, editing out structures with especially high R factor and projection structures.

To calculate the H atom positions, we have imposed a C–H distance of 1.08 Å throughout[3] and used the following protocol:

(a) For methyl groups, compute one approximate C–C–C–H torsion angle, ω, using X-ray H atom positions and use this to build a methyl group with angle C–C–H = 109.47° and torsion angles ω, ω + 120, ω + 240; if no X-ray hydrogens are available, use ω = 60°. As a side result, it appears that in aliphatic environments ω is near to 60° in most cases, while a spread of values is observed in methyl substituents at aromatic rings.

(b) For methylene groups, use two H atoms, in the plane bisecting the C–C–C angle and perpendicular to the C–C–C plane. C–C–H angles are computed by requiring orthogonality of hybrids at carbon.[3a,4a]

(c) For methyne hydrogens, renormalize the C–H distance, starting from X-ray hydrogen positions; if these are not available, compute an approximate position with no C–C–H angles <100°.

(d) For aromatic ring or ethylenic H atoms, calculate the positions in the C–C–C plane, on the bisector of the C–C–C angle.

In a few remaining cases, ad hoc procedures were adopted, based on reasonable geometric conditions.

Kinetics of Electron-Transfer Reactions of Hydroquinones and Ascorbic Acid with 1-Phenyl-3-pyrazolidone Radicals
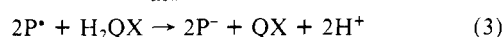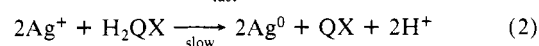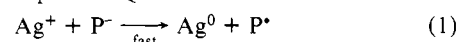
Michael P. Youngblood

Contribution from the Paper and Reversal Chemistry Laboratory, Eastman Kodak Company, Rochester, New York 14650. Received June 8, 1988

Abstract: The kinetics of oxidation of four hydroquinones and ascorbic acid by 1-phenyl-3-pyrazolidone radicals have been examined in aqueous solution from pH 6.5 to 9.5. For the hydroquinones, the kinetics are markedly autocatalytic unless sulfite is present in the solutions. The autocatalysis is apparently due to accumulation of a significant quantity of semiquinone formed via reproportionation of the quinone product with unreacted hydroquinone. If present in sufficient concentration, sulfite eliminates autocatalysis by scavenging quinone, and the kinetics are first-order in each reactant. The kinetic results suggest that the electron transfer from hydroquinone to the radical to form semiquinone is rate-limiting. In the case of ascorbic acid, autocatalysis is not observed, and the kinetics are first-order in oxidant and reductant. The kinetic dependence on pH permits the resolution of bimolecular rate constants for oxidation of the fully ionized and the singly protonated reductants. The correlation of these rate constants with thermodynamic driving force is in agreement with the Marcus theory.

It is well-known that photographic developers containing a combination of a hydroquinone (H_2QX) and a 1-aryl-3-pyrazolidone (HP) exhibit development rates many times greater than is seen when either agent is used alone.[1] This so-called superadditivity has been studied extensively. It is widely accepted that superadditivity is largely due to a regeneration mechanism in which the pyrazolidone anion (P^-) is the predominant agent

for reduction of silver ions and the hydroquinone serves primarily to reduce the oxidized pyrazolidone (radical) to its active form (eq 1–3, where the quinone QX is the two electron oxidation

$$Ag^+ + P^- \xrightarrow[\text{fast}]{} Ag^0 + P^\bullet \tag{1}$$

$$2Ag^+ + H_2QX \xrightarrow[\text{slow}]{} 2Ag^0 + QX + 2H^+ \tag{2}$$

$$2P^\bullet + H_2QX \rightarrow 2P^- + QX + 2H^+ \tag{3}$$

product derived from H_2QX, and $P^\bullet$ is pyrazolidone radical).

---

(1) Levenson, G. I. P. *Photogr. Sci. Eng.* **1969**, *13*, 299.

Regeneration of the pyrazolidone circumvents development inhibition by the radical. The mechanism was first proposed by Levenson to explain the superadditivity of hydroquinone and *p*-(methylamino)phenol[2] and has since been invoked by numerous authors[3-6] to explain the hydroquinone/1-aryl-3-pyrazolidone superadditivity.

Jaenicke et al. have demonstrated the close analogy between the regeneration mechanism (eq 1-3) and the catalytic electrode processes.[7,8] In the presence of excess sulfite, hydroquinone is only very slowly oxidized at silver or gold electrodes because sulfite inhibits the electrooxidation of hydroquinone by adsorbing to the electrode surface. If 1-phenyl-3-pyrazolidone is added to an alkaline solution of hydroquinone and sulfite, a catalytic current, corresponding to the oxidation of hydroquinone, is observed at the redox potential of 1-phenyl-3-pyrazolidone. Oxidation of 1-phenyl-3-pyrazolidone is not inhibited by sulfite. The catalytic current is due to oxidation of the pyrazolidone at the electrode to generate a radical, which is rapidly converted back to the reduced form via reaction with hydroquinone in the solution adjacent to the electrode surface.

The electrochemical studies of Jaenicke et al. have provided an indirect means of measuring the rates of reduction of pyrazolidone radicals by hydroquinones and other reducing agents. In this paper, the kinetics of reduction of the radical forms of 5-methyl-1-phenyl-3-pyrazolidone (**1•**) and 4-methyl-4-(hydrox-

$$1 : R^1=R^2=H, R^3=CH_3$$
$$2 : R^1=CH_3, R^2=CH_2OH, R^3=H$$
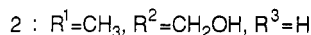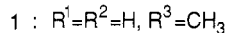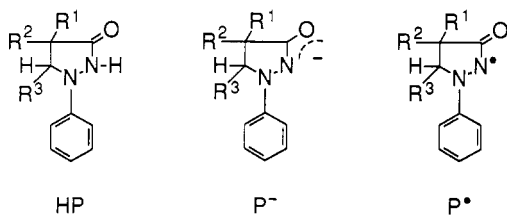
ymethyl)-1-phenyl-3-pyrazolidone (**2•**) by several hydroquinones and by ascorbic acid are described. The kinetics have been measured directly by utilizing a novel in situ preparation of the radicals.

Experimental Section

For kinetic measurements, a Dionex Model D-110 stopped-flow spectrophotometer interfaced to a Motorola M6800 microprocessor was used. Observed rate constants and stoichiometry were determined by mixing a solution containing either **1** or **2**, sodium sulfite, the reductant (a hydroquinone or ascorbic acid), and KCl with a solution containing potassium ferricyanide, a buffer, and KCl. The concentration of the radicals of **1** or **2**, formed in situ via oxidation of the corresponding parent pyrazolidone by ferricyanide (see below), was monitored by the absorbance at 500 nm. For kinetic and stoichiometric measurements, concentrations were 1.0×10^{-4} M for pyrazolidone (**1** or **2**) and ferricyanide, 0.010–0.050 M for sulfite, 0.010–0.020 M for each buffer, and 0.10 M for KCl. For rate determinations, reductant concentrations were 1.0×10^{-3} M or greater, but they ranged from 1.0×10^{-5} to 2.0×10^{-4} M in the stoichiometric experiments. For the reported rate constants, the ionic strength was 0.20 ± 0.05, depending on buffer and sulfite concentration. The temperature was held constant at 25.0 ± 0.1 °C. The following buffers were used: malonic acid (pH 5.5–6.0), 2-(4-morpholino)-ethanesulfonic acid (pH 6.0–6.8), 4-(2-hydroxyethyl)-1-piperazine-ethanesulfonic acid (pH 7.0–8.0), 4-(2-hydroxyethyl)-1-piperazine-propanesulfonic acid (pH 8.0–8.5) and sodium borate (pH 8.5–9.5).

The acid-dissociation constants for hydroquinone-2,5-disulfonate and methylhydroquinone were measured by spectrophotometric titration with

(2) Levenson, G. I. P. *Photogr. J.* **1949**, *89B*, 13.
(3) Axford, A. J.; Kendall, J. D. *J. Photogr. Sci.* **1954**, *2*, 1.
(4) Willems, J. F. *Photogr. Sci. Eng.* **1971**, *15*, 213.
(5) Levenson, G. I. P.; Twist, P. J. *J. Photogr. Sci.* **1978**, *26*, 44.
(6) Van Veelen, G. F.; Ruyschaert, H. *Photogr. Sci. Eng.* **1960**, *4*, 129.
(7) Jaenicke, W.; Kobayashi, H. *J. Photogr. Sci.* **1983**, *31*, 69.
(8) Jaenicke, W.; Kobayashi, H.; Kawashima, S.; Ohno, T.; Mizusawa, S. *J. Imaging Sci.* **1986**, *30*, 121.

Table I. Thermodynamic Properties of the Reactants[a]

compound	E^0	E^0_{alk}	pK_{a1}	pK_{a2}
1	0.737^b	0.146	9.99^b	
2	0.689^b	0.136	9.36^b	
hydroquinone	0.699^c	0.065	9.91^c	11.56^c
methylhydroquinone	0.644^c	−0.012	10.14^d	12.11^d
hydroquinonesulfonate	0.767^c	0.132	9.57^c	11.9^c
hydroquinone-2,5-disulfonate	0.851^e	0.197	9.49^d	11.91^d
ascorbic acid			4.04^c	11.34^c

$^a E^0_{alk}$ = reduction potential for doubly deprotonated hydroquinone/quinone couple (two-electron) or pyrazolidone anion/radical couple (one-electron). $^b E^0_{alk}$ calculated from E^0 (standard reduction potential at unit hydrogen ion activity) and pK_a values. $T = 25$ °C in all cases. ^{b} Brown, E. R., unpublished data. $\mu = 0.18$. ^{c} Lee, W. E.; Brown, E. R. In *The Theory of the Photographic Process*; James, T. H., Ed.; MacMillan: New York, 1977; pp 300–311. (For pK_a values: $\mu = 0.1$ (hydroquinone, ascorbic acid); $\mu = 0.375$ (hydroquinonesulfonate)). ^{d} This work, $\mu = 0.1$. ^{e} Mentasti, E.; Pelizzetti, E. *Int. J. Chem. Kin.* **1977**, *9*, 215.

NaOH at 25 °C in 0.10 M KCl. The spectra of oxygen-free solutions of the hydroquinones were measured as a function of pH with a Perkin-Elmer 320 UV–visible spectrophotometer.

The pyrazolidones **1** and **2** are not commercially available, but purified samples were obtained from Eastman Kodak Co. Hydroquinone and methylhydroquinone from Kodak Laboratory Chemicals were used as received. The potassium salts of hydroquinonesulfonate and hydroquinone-2,5-disulfonate were used as received from Aldrich. The buffers (see above) were used as received from Kodak Laboratory Chemicals.

Results and Discussion

Reactants and Their Redox Potentials. The kinetics of six reactions were examined. The oxidant was the radical of either **1** or **2**, and the reductant was one of four hydroquinones or ascorbic acid. Table I lists the reactants, their half-cell reduction potentials, and the pK_as of the reduced form of each couple. The pK_a values for hydroquinonedisulfonate and methylhydroquinone were determined by spectrophotometric titration; the other values in Table I were taken from the literature or calculated from published data. The potentials E^0_{alk} are pH-independent values for the reduced forms in their fully ionized states. Given the pH-independent potential (E^0_{alk}) and the pK_as, the formal potential at any pH can be expressed as in eq 4a (for hydroquinones) or 4b (for pyrazo-

$$E_f = E^0_{alk} = \frac{0.0591}{2} \log \left(\frac{K_{a1}K_{a2} + K_{a1}[H^+] + [H^+]^2}{K_{a1}K_{a2}} \right) \quad (4a)$$

$$E_f = E^0_{alk} + 0.0591 \log \left(\frac{K_{a1} + [H^+]}{K_{a1}} \right) \quad (4b)$$

lidones). The formal redox potential for a given redox reaction at a given pH, E_f(reaction), is given simply by E_f(ox) − E_f(red). Several of the reactions examined in this study have a negative or very small overall driving force. The kinetic measurements of these reactions required a product scavenger to drive them to completion. Sulfite addition to the quinone products provides a means of driving the thermodynamically unfavorable reactions to completion. As discussed below, the scavenging of quinones by sulfite has a major effect on the kinetic nature of the redox reactions.

In Situ Preparation of Pyrazolidone Radicals. Pyrazolidone radicals are conveniently generated via oxidation of the parent pyrazolidone by a stoichiometric amount of ferricyanide. However, the radicals disproportionate with half-lives ranging from a few seconds to 10 min, depending on the structure and initial concentration of the pyrazolidone.[9-11] The instability of the radicals presents an experimental problem in preparing solutions for kinetic

(9) Lee, W. E.; Miller, D. W. *Photogr. Sci. Eng.* **1966**, *10*, 192.
(10) Battaglia, C. J.; Lee, W. E.; Miller, D. W.; Allen, E. S.; Glover, W. *J. Photogr. Sci. Eng.* **1970**, *14*, 397.
(11) Castellan, A.; Massetti, F.; Mazzucato, U.; Vianello, E. *J. Photogr. Sci.* **1966**, *14*, 164.

Figure 1. Absorbance versus time trace showing the formation and decay of 1.0×10^{-4} M **2**° in the absence (A) and presence (B) of hydroquinone $(1.0 \times 10^{-3}$ M) at pH 7.0.
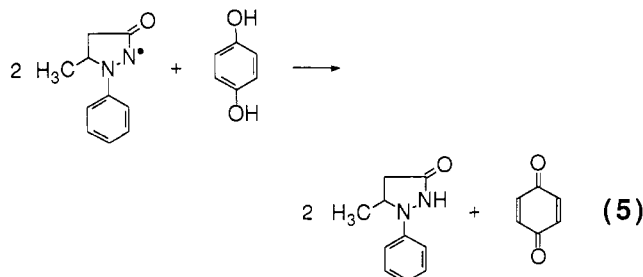
studies. Fortunately, it was found that pyrazolidone radicals can be generated by ferricyanide oxidation even in the presence of a large excess of hydroquinones. Preliminary experiments revealed that the rate of oxidation of **2** by ferricyanide is approximately 3 orders of magnitude faster than the corresponding oxidation of hydroquinone over the pH range 6–9.5. Figure 1 shows the consequences of this rate difference at pH 7.0. The radical formation is monitored by the absorbance at 500 nm. The radical is generated quantitatively by an equimolar amount of ferricyanide in approximately 0.5 s. The absorbance/time trace at times shorter than 0.5 s for the case where a 10-fold excess of hydroquinone (0.0010 M) was present is essentially superimposable with the trace in which hydroquinone was absent. This indicates that the oxidation of **2** by ferricyanide is fast enough that no ferricyanide is consumed by the excess hydroquinone. Also, the generation of the radical is much faster than the subsequent reduction by hydroquinone. The absorbance values at time zero in all the kinetic experiments to be described below suggest that in all cases radicals (**1**° or **2**°) are quantitatively generated prior to their reduction.

Stoichiometry. With use of the in situ preparation of radicals described in the preceding section, the reaction of the radical of **1** with hydroquinone was monitored spectrally to determine the stoichiometry. Solutions were prepared with varying ratios of hydroquinone to **1** (the concentration of **1** was constant at 0.20 mM). These solutions were subsequently mixed with a 0.20 mM solution of potassium ferricyanide buffered at pH 9.10 with 0.025 M borate. The generation of **1**° was complete within the mixing time (5 ms) and the reaction of the radical with hydroquinone was much faster than the disproportionation at this pH. The absorbance was measured after the rapid reaction with hydroquinone was complete but before any significant disproportionation had occurred. When plotted against the molar ratio of hydroquinone to radical, the absorbance data (Figure 2) show that the stoichiometry follows eq 5.

$$2 \; H_3C\underset{\underset{\text{Ph}}{|}}{\overset{O}{\underset{N-N°}{\diagup}}} + \overset{OH}{\underset{OH}{\bigcirc}} \longrightarrow$$

$$2 \; H_3C\underset{\underset{\text{Ph}}{|}}{\overset{O}{\underset{N-NH}{\diagup}}} + \overset{O}{\underset{O}{\bigcirc}} \qquad (5)$$

The curvature in Figure 2 in the vicinity of the end point reflects reversibility in the redox reaction. This is expected, as the reaction driving force is only 38 mV at pH 9.10. The mole ratio experiment was repeated with 0.010 M sulfite in the solution of **1** and hy-
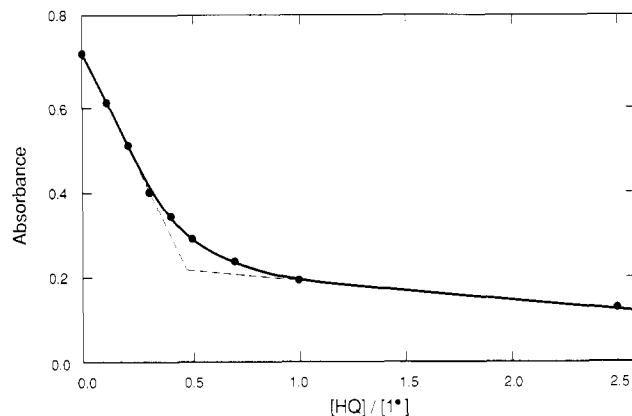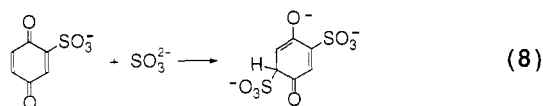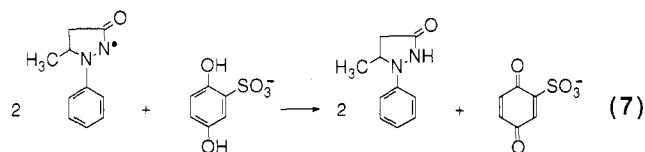

Figure 2. Absorbance versus mole ratio for oxidation of hydroquinone by **1**°, pH 9.10.

droquinone. The sulfite was added to scavenge benzoquinone by reductive addition (eq 6), thus making the redox reaction irreversible. The rate constant for sulfite addition to benzoquinone

$$\overset{O}{\underset{O}{\bigcirc}} + SO_3^{2-} \longrightarrow \overset{OH}{\underset{O_-}{\bigcirc}}SO_3^- \qquad (6)$$
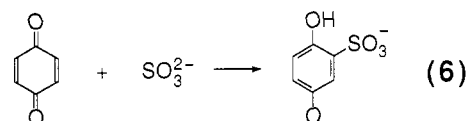
$(7.7 \times 10^4 \; M^{-1} \; s^{-1})^{12}$ is large enough that 0.010 M sulfite should efficiently scavenge the quinone. The resulting absorbance/mole ratio plot showed that more than 2 mol of radical were consumed per mole of hydroquinone. In the absence of hydroquinone, no appreciable reaction took place between the radical and sulfite during the time scale of interest. Hence, the increased consumption of radical was apparently due to its reduction by the hydroquinonemonosulfonate formed from sulfite addition to benzoquinone (eq 7 and 8). The reduction of **1**° by hydro-

$$2 \; H_3C\underset{\underset{\text{Ph}}{|}}{\overset{O}{\underset{N-N°}{\diagup}}} + \overset{OH}{\underset{OH}{\bigcirc}}SO_3^- \longrightarrow 2 \; H_3C\underset{\underset{\text{Ph}}{|}}{\overset{O}{\underset{N-NH}{\diagup}}} + \overset{O}{\underset{O}{\bigcirc}}SO_3^- \qquad (7)$$

$$\overset{O}{\underset{O}{\bigcirc}}SO_3^- + SO_3^{2-} \longrightarrow \underset{-O_3S}{\overset{O^-}{\underset{O}{\bigcirc}}}\overset{SO_3^-}{\underset{H}{}} \qquad (8)$$

quinonemonosulfonate is thermodynamically unfavorable, but is apparently driven to completion by the addition of sulfite to benzoquinonemonosulfonate. Kinetic studies of the reaction of benzoquinonemonosulfonate with sulfite indicate that nucleophilic addition to form the 1,4-adduct (eq 8) is rapid and that the adduct enolizes to hydroquinonedisulfonate in a slower subsequent step.[13] The stoichiometric and kinetic results reported below for the oxidation of hydroquinonemonosulfonate and hydroquinonedisulfonate support the assumption that the 1,4-adduct depicted in eq 8 does not enolize to hydroquinonedisulfonate on the time scales of the redox reactions. Given eq 5–8, it is apparent that with excess sulfite present as much as 4 mol of radical can be consumed by each mole of hydroquinone.

The stoichiometry of the reduction of **2**° by hydroquinone was examined by the mole ratio method described previously. The results were quite similar to those found for the correponding reduction of **1**°. In the absence of sulfite, the absorbance–mole ratio plot showed approximately 2 mol of radical consumed per mole of hydroquinone. The plot exhibited even more curvature than in the case of **1**° because E_f (reaction) is zero at pH 9.10.

(12) Youngblood, M. P. *J. Org. Chem.* **1986**, *51*, 1981.
(13) Youngblood, M. P., to be submitted for publication.
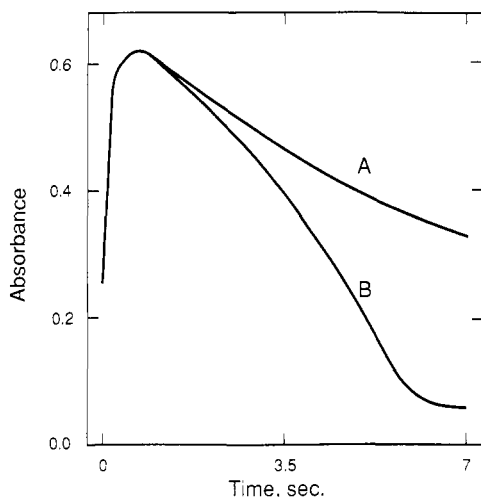
Figure 3. Effect of sulfite on the kinetic trace for the oxidation of hydroquinone (1.0×10^{-3} M) by $1^{\bullet}$ (initially 1.0×10^{-4} M) at pH 7.84: A, 0.005 M sulfite; B, no sulfite.
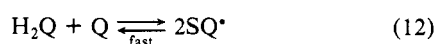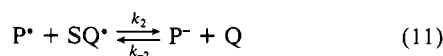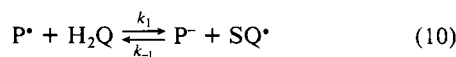
The presence of sulfite again increased the stoichiometry owing to steps analogous to eq 5–8.

The reduction of $2^{\bullet}$ by hydroquinonemonosulfonate is thermodynamically uphill (−40 mV at pH 9.90). Hence, in the absence of sulfite, the reduction of the radical by hydroquinone monosulfonate did not occur to a significant extent at pH 9.90. However, when conducted in the presence of 0.050 M sulfite at pH 9.90 (0.050 M borate), the mole ratio experiment yields a plot that clarly shows that 2 mol of $2^{\bullet}$ are consumed by each mole of hydroquinonemonosulfonate. This suggests that the unfavorable reaction is driven to completion by sulfite, which scavenges the p-benzoquinonemonosulfonate (eq 8).

Kinetics of Reduction of $1^{\bullet}$ by Hydroquinone. Figure 3 shows kinetic traces observed when $1^{\bullet}$ is generated in the presence of excess hydroquinone. The kinetics in the absence of sulfite are clearly autocatalytic: the rate of radical disappearance increases with time. Sulfite has a significant effect on the curve shape of the kinetic trace (Figure 3). In the presence of 0.0050 M sulfite, the autocatalytic behavior is not observed, and the overall rate is much slower as a result. Note that the initial rate of radical disappearance is essentially independent of sulfite, suggesting that the only role of sulfite is the prevention of autocatalysis. The presence of 0.010 M or more sulfite causes the kinetics to be first-order, provided the hydroquinone is in at least a 10-fold excess over the radical and the solutions are well buffered. Under these conditions the experimental rate law is given by eq 9.

$$\frac{d[P^{\bullet}]}{dt} = k_{obsd}[P^{\bullet}] \tag{9}$$

The stoichiometry experiments described above provide evidence that 0.010 M sulfite rapidly scavenges p-benzoquinone as it is formed from oxidation of hydroquinone by $1^{\bullet}$. The suppression of p-benzoquinone accumulation also provides an explanation of the effect of sulfite on the kinetic behavior of the redox reactions (eq 10–13). In eq 10–13 the ionization of hydroquinone is ignored

$$P^{\bullet} + H_2Q \underset{k_{-1}}{\overset{k_1}{\rightleftharpoons}} P^- + SQ^{\bullet} \tag{10}$$

$$P^{\bullet} + SQ^{\bullet} \underset{k_{-2}}{\overset{k_2}{\rightleftharpoons}} P^- + Q \tag{11}$$

$$H_2Q + Q \underset{fast}{\rightleftharpoons} 2SQ^{\bullet} \tag{12}$$

$$Q + SO_3^{2-} \rightarrow HQS \tag{13}$$

for simplicity. The effect of hydroquinone ionization is considered below in the discussion of pH dependence.

In the absence of sulfite, the p-benzoquinone product reacts with the excess hydroquinone to generate semiquinone (eq 12), which has often been shown to be a more powerful reductant than
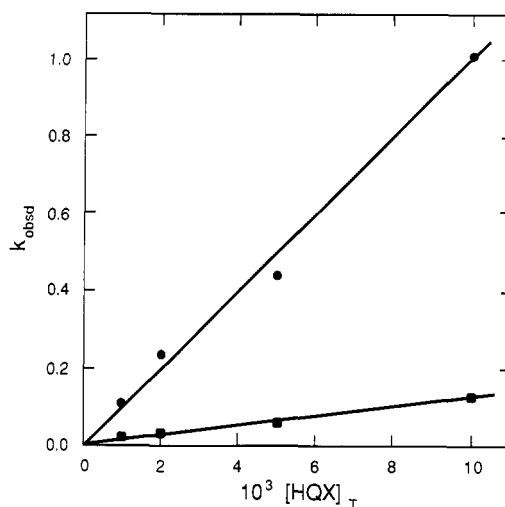
Figure 4. Kinetic dependence on excess reductant concentration for the oxidation of hydroquinone by $1^{\bullet}$ at pH 7.7 ($\bullet$) and hydroquinone-2,5-disulfonate by $2^{\bullet}$ at pH 7.55 ($\blacksquare$).

hydroquinone.[14,15] As the reaction progresses, the concentration of semiquinone increases and the reaction rate consequently increases. Thus, semiquinone functions as an autocatalyst. However, in the presence of sufficient sulfite, p-benzoquinone is apparently removed via sulfonation rapidly enough that semiquinone formation via reproportionation (eq 13) is suppressed.

If p-benzoquinone is effectively scavenged by sulfite, the rate of the redox reaction should be independent of sulfite concentration. This is observed at sulfite levels greater than 0.010 M. The sulfite-independent rates suggest that neither eq 12 nor eq 13 is kinetically important, leaving eq 10 and 11 to be considered in deriving the expected rate law. Given that the quinone is effectively scavenged, the reverse rate in eq 11 should be negligible. Assuming that the semiquinone is formed only in steady-state concentration and that $k_{-2}[P][Q] \ll k_1[P^{\bullet}][H_2Q]$ leads to a rate law given by eq 14. The subscript T denotes the total concen-

$$\frac{d[P^{\bullet}]}{dt} = \frac{2k_1k_2[P^{\bullet}]^2[H_2Q]_T}{k_{-1}[P^-] + k_2[P^{\bullet}]} \tag{14}$$

tration of various ionized forms of hydroquinone. If eq 10 is rate-limiting, eq 14 simplifies further to eq 15. If eq 11 were

$$\frac{d[P^{\bullet}]}{dt} = 2k_1[P^{\bullet}][H_2Q]_T \tag{15}$$

rate-limiting, the derived rate law would be second-order in radical concentration, contrary to the observed first-order behavior.

When comparing eq 9 and 15, it is apparent that according to the proposed mechanism the pseudo-first-order rate constant, k_{obsd}, is given by eq 16. The dependence of k_{obsd} upon excess hydroquinone concentration was confirmed to be first-order (Figure 4), in accordance with eq 16.

$$k_{obsd} = 2k_1[H_2Q]_T \tag{16}$$

It should be noted that the increased consumption of radical that was observed when the mole ratio stoichiometry experiments were carried out in the presence of sulfite apparently does not affect the kinetics described here. The fact that a 10-fold excess of hydroquinone over $1^{\bullet}$ was always used probably makes the kinetic contribution of the hydroquinonemonosulfonate product insignificant.

Reduction of $2^{\bullet}$ by Hydroquinone and Substituted Hydroquinones. The kinetics of reduction of $2^{\bullet}$ by hydroquinone, hydroquinonemonosulfonate, hydroquinonedisulfonate, and methylhydroquinone were qualitatively similar to those observed for

(14) Clemmer, J. D.; Hogaboom, G. K.; Holwerda, R. A. *Inorg. Chem.* **1979**, *18*, 2567.
(15) Pelizzetti, E.; Mentasti, E.; Balocchi, C. *J. Phys. Chem.* **1976**, *80*, 2979.

Table II. Resolved Bimolecular Rate Constants[a]

oxidant	reductant[b]	$K_b{}^c$	k_b, M^{-1} s^{-1}	$K_c{}^c$	k_c, M^{-1} s^{-1}
2•	HQDS	1.8×10^{-9}	$(5 \pm 2) \times 10^2$	0.75	$(6 \pm 1) \times 10^6$
2•	HQS	4.7×10^{-8}	$(9 \pm 4) \times 10^2$	7.5	$(1.4 \pm 0.3) \times 10^7$
2•	HQ	9.1×10^{-7}	$(2.6 \pm 0.7) \times 10^3$	33	$(2.6 \pm 0.4) \times 10^7$
1•	HQ	1.3×10^{-6}	$(4 \pm 1) \times 10^3$	48	$(3.0 \pm 0.6) \times 10^7$
2•	MeHQ	7.1×10^{-6}	$(2.8 \pm 0.4) \times 10^4$	4.6×10^2	$(1.1 \pm 0.3) \times 10^8$
2•	AA		$(9.5 \pm 0.8) \times 10^2$		$(9.0 \pm 0.4) \times 10^6$

[a] $T = 25$ °C, $\mu = 0.2$. Errors given are 95% confidence limits. [b]HQDS = hydroquinone-2,5-disulfonate; HQS = hydroquinonesulfonate; HQ = hydroquinone; MeHQ = methylhydroquinone; AA = ascorbic acid. [c]K_b and K_c calculated from eq 27 and 24, respectively, with K_s values of 66 for HQDS (Mentasti, E.; Pelizzetti, E. *Int. J. Chem. Kin.* **1977**, *9*, 215), 41 for HQS; 4.2 for HQ, 2.0 for MeHQ (Bishop, C. A.; Tong, L. K. *J. J. Am. Chem. Soc.* **1965**, *87*, 501). $pK_{a2}{}^{SQ}$ estimates are as follows: 3.3 for HQDS, 3.7 for HQS, 4.0 for HQ, 4.5 for MeHQ (ref 15).
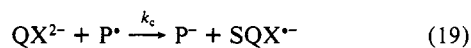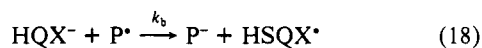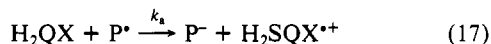
the reduction of **1•** by hydroquinone. The reduction of **2•** by hydroquinonemonosulfonate and by hydroquinonedisulfonate did not occur to an appreciable extent in the absence of sulfite. With hydroquinone or methylhydroquinone as reductants, the kinetics were autocatalytic in the absence of sulfite and became cleanly first-order in radical and in reductant if sulfite was present at 0.010 M or greater. Thus, the kinetics of each reaction appears to be consistent with the mechanism in eq 10–13 and with rate equations in eq 14–16.

Kinetic Dependence on pH. The rates of reduction of **1•** by hydroquinone and of **2•** by hydroquinone, hydroquinonemonosulfonate, hydroquinonedisulfonate, and methylhydroquinone were measured as a function of pH. Sulfite was present in all cases and the hydroquinones were in a 10-fold or greater excess over the initial concentration of radical. The kinetics were first-order in radical over the pH range examined.

In the preceding mechanistic discussion regarding eq 10–16, the arguments were simplified by ignoring the extent of ionization of the hydroquinones. In fact, however, the rate constant k_1 is a composite of rate constants for each of the three forms of hydroquinone (H_2QX, HQX^-, and QX^{2-}).

An apparent second-order rate constant, k_{app}, may be defined by the slope of k_{obsd} vs reductant concentration (or by $k_{obsd}/[\text{reductant}]_T$) for each pH. The dependence of log k_{app} on pH is illustrated for the reaction of **2•** with hydroquinone and with hydroquinone monosulfonate in Figure 5. For each of these reactions there is a linear dependence of log k_{app} on pH having a slope of 2.0 above pH 8. Below pH 8 the curves change to a slope of approximately unity. The other reactions gave the same general behavior.

A mechanistic interpretation of the experimental pH dependence requires the derivation of an expanded rate expression for k_1 that accounts for the different reactivities of each of the forms of hydroquinone. Assuming that H_2QX, HQX^-, and QX^{2-} are in rapid equilibrium and that each reacts with the oxidant in three separate pathways (eq 17–19), k_1 is given by eq 20, where k_a, k_b, and k_c are bimolecular rate constants for each pathway and K_{a1} and K_{a2} are the acid-dissociation constants for H_2QX.

$$H_2QX + P^\bullet \xrightarrow{k_a} P^- + H_2SQX^{\bullet+} \qquad (17)$$

$$HQX^- + P^\bullet \xrightarrow{k_b} P^- + HSQX^\bullet \qquad (18)$$

$$QX^{2-} + P^\bullet \xrightarrow{k_c} P^- + SQX^{\bullet-} \qquad (19)$$

$$k_1 = \frac{k_a[H^+]^2 + k_bK_{a1}[H^+] + k_cK_{a1}K_{a2}}{[H^+]^2 + K_{a1}[H^+] + K_{a1}K_{a2}} \qquad (20)$$

All the data were collected at pH <9.5, where the $[H^+]^2$ term in the denominator of eq 20 is dominant for the hydroquinones. The $K_{a1}K_{a2}$ term is negligible over that pH range and the $K_{a1}[H^+]$ term contributes only slightly. To agree with the experimentally observed pH dependence, the $k_a[H^+]^2$ term in the numerator of eq 20 must be negligible compared with the other two terms. Hence, eq 20 may be simplified to eq 21. The change from a

$$k_1 = \frac{k_bK_{a1}[H^+] + k_cK_{a1}K_{a2}}{[H^+]^2 + K_{a1}[H^+]} \qquad (21)$$

$[H^+]^{-1}$ to a $[H^+]^{-2}$ kinetic dependence with increasing pH (Figure
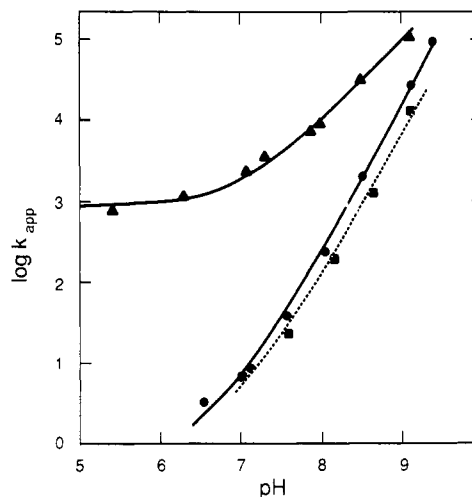

Figure 5. Kinetic dependence on pH for the oxidation of hydroquinone (●), hydroquinonesulfonate (■), and ascorbic acid (▲). See the text for an explanation of the calculated curves.

5) can then be explained as a transition from the kinetic prevalence of the singly deprotonated hydroquinone at lower pH ($k_bK_{a1}[H^+]$ $\gg$ $k_cK_{a1}K_{a2}$) to the prevalence of the doubly deprotonated form at higher pH ($k_bK_{a1}[H^+]$ $\ll$ $k_cK_{a1}K_{a2}$).

Nonlinear-regression analysis was used to fit the experimental data to eq 22. Values of K_{a1} and K_{a2} from Table I were used as constants in the regression, whereas k_b and k_c were treated as

$$k_{obsd} = 2\left(\frac{k_bK_{a1}[H^+] + k_cK_{a1}K_{a2}}{[H^+]^2 + K_{a1}[H^+]}\right)[H_2QX]_T \qquad (22)$$

adjustable parameters. The curves for the hydroquinones in Figure 5 were calculated from eq 22 ($k_{app} = k_{obsd}/[\text{reductant}]_T$) with the values of k_b and k_c obtained from the regression analysis. Table II lists the values of k_b and k_c for each of the reactions examined.

Kinetics of the Reduction of 2• by Ascorbic Acid. The **2•** was generated in the presence of ascorbic acid by ferricyanide oxidation of **2**, as described above for the hydroquinone reactions. A mole ratio plot indicated that 2 mol of **2•** are reduced by each mole of ascorbic acid. The reversible redox potential of ascorbic acid is not accurately known because the two electron oxidized form, dehydroascorbic acid, undergoes a very rapid irreversible hydration reaction.[16] Polarographic $E_{1/2}$ values have been reported in a number of papers, but these numbers are more negative than the reversible potential owing to the chemical irreversibility of the electrode reaction. Like the electrooxidation, homogeneous redox reactions of ascorbic acid are irreversible.

The kinetics of reduction of **2•** by ascorbic acid were shown to be first-order with respect to both reactants. The pH dependence is shown in Figure 5. Over the pH range examined, the kinetics show a transition from a pH-independent rate to a $[H^+]^{-1}$ dependence. The kinetic dependences are consistent with a mechanism and rate law analogous to those for the hydroquinones. The pH profile differs from the hydroquinone curves in Figure 5, owing to the wide separation in pK_{a1} (4.04) and pK_{a2} (11.34)

(16) Perone, S. P.; Kretlow, W. J. *Anal. Chem.* **1966**, *12*, 1760.

1848 *J. Am. Chem. Soc., Vol. 111, No. 5, 1989*

Youngblood

for ascorbic acid.[17] Over the pH range examined, only the $K_{a1}[H^+]$ term in the denominator of eq 20 is significant. Hence, for ascorbic acid as the reductant, eq 20 simplifies to eq 23.

$$k_{app} = 2k_1 + 2k_b + 2k_c K_{a2}/[H^+] \qquad (23)$$

Nonlinear-regression analysis yields values of $(9.5 \pm 0.8) \times 10^2$ and $(9.0 \pm 0.4) \times 10^6$ for k_b and k_c, respectively. The solid curve in Figure 5 was calculated with these values in eq 23.

An electrochemical study reported by Jaenicke et al. yielded apparent rate constants of 5.1×10^4 and 2.9×10^4 M^{-1} s^{-1} (at pH 9.0) for the oxidation of hydroquinone and ascorbic acid, respectively, by 1-phenyl-3-pyrazolidone radical.[8] These values are similar to k_{app} (at pH 9.0) for oxidation of hydroquinone and ascorbic acid by **2•** in the present study. The electrochemical studies[7,8] were not done over a sufficiently wide range of reaction conditions to allow values of k_a, k_b and k_c to be resolved or to test agreement with the observed rate expressions given by eq 9, 16, and 21.

Correlation of Rate Constants for Hydroquinone Oxidations with Thermodynamic Driving Force. The equilibrium constants for the one-electron oxidation of the fully ionized hydroquinones by both radicals (as written in eq 19), K_c, have been calculated with eq 24, where K_{2e} and K_s are the equilibrium constants for reactions 25 and 26, respectively. K_{2e} values were calculated from the

$$K_c = (K_{2e}K_s)^{1/2} \qquad (24)$$

$$QX^{2-} + 2P• \rightleftharpoons QX + 2P^- \qquad (25)$$

$$QX^{2-} + QX \rightleftharpoons 2SQX•^- \qquad (26)$$
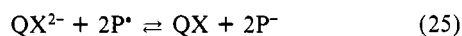
alkaline half-cell potentials for each reactant pair (Table I). Values of K_s for each of the hydroquinones have been reported in the literature (see footnotes, Table II). The equilibrium constants for the one-electron oxidation of singly protonated hydroquinones, K_b, were calculated from eq 27, where K_{a2}^{SQ} is the

$$K_b = \frac{(K_{2e}K_s)^{1/2}K_{a2}}{K_{a2}^{SQ}} \qquad (27)$$

acid-dissociation constant for HSQX•. Values of K_{a2}^{SQ} for several semiquinones and linear plots of E^0 versus pK_{a2}^{SQ} from which unknown values may be estimated, have been cited by Pelizzetti et al.[15] The values range from 3.3 for 2,5-semiquinonedisulfonate to 4.5 for methylsemiquinone (see footnotes, Table II).

According to the Marcus theory of electron transfer in its simplest form, the rate constant for an outer-sphere electron-transfer reaction (k_{et}) is related to the thermodynamic equilibrium constant for the reaction (K_{eq}) by eq 28 and 29.[18] The other

$$k_{et} = (k_{11}k_{22}K_{eq}f)^{1/2} \qquad (28)$$

$$\log f = (\log K_{eq})^2 / [4 \log (k_{11}k_{22}/Z^2)] \qquad (29)$$

parameters in eq 28 and 29 are the self-exchange rate constants, k_{11} and k_{22}, for each reactant and the collision frequency, Z, generally assumed to be 10^{11} s^{-1}. The derivation of eq 28 and 29 assumes that the Coulombic work terms in the electron-transfer and self-exchange processes are either similar, so as to cancel in the mathematical treatment, or negligibly small. In the present case this is reasonable, given the charges involved and the relatively high ionic strength of the medium.

Equations 28 and 29 were used to correlate k_c with K_c and k_b with K_b. Holwerda et al.[14] and McAuley et al.[19] have argued that the self-exchange rates of hydroquinone/semiquinone systems are not affected by the degree of protonation or by substitution on the hydroquinone ring. Self-exchange rate constants of approximately 5×10^7 M^{-1} s^{-1} have been reported by these authors for H_2QX/H_2SQX^+ and $HQX^-/HSQX$. Assuming this value for
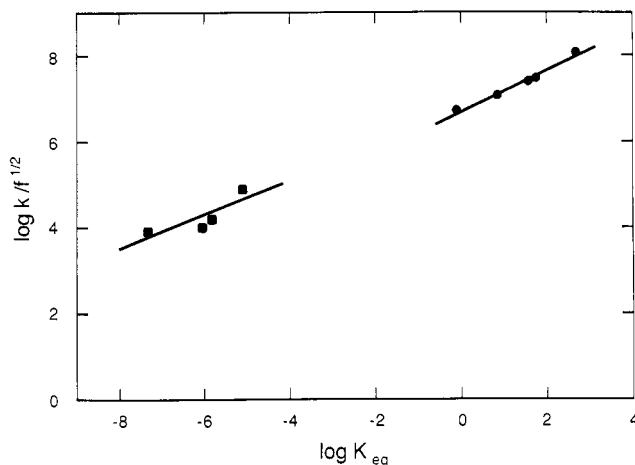

Figure 6. Marcus free energy correlation for the oxidation of singly protonated (■) and fully ionized (●) hydroquinones by **1•** and **2•**.

k_{11}, values of k_{22} and f were calculated by successive approximations from eq 28 and 29 with k_c and K_c from Table II. The value of k_{22} from these calculations is essentially constant at $(6 \pm 2) \times 10^5$ M^{-1} s^{-1}, whereas f values range from 0.62 to 1.0. A plot (Figure 6) of $\log (k_c/f^{1/2})$ vs $\log K_c$ yields a slope of 0.49 ± 0.05, in agreement with the slope predicted by eq 28. The intercept of the line yields a value of $k_{22} = 8 \times 10^5$ M^{-1} s^{-1} for the pyrazolidone anion/radical self-exchange, assuming the value of k_{11} quoted above.

The correlation of k_b with K_b (Figure 6) shows considerable scatter. This it not unreasonable given that the k_b values are less precise than k_c and that rather crude estimates of K_{a2}^{SQ} were used in calculating K_b. Assuming a value of 5×10^7 M^{-1} s^{-1} for k_{11} ($HQX^-/HSQX$ self exchange), values of f and k_{22} were calculated by successive approximation using k_b and K_b from Table II. For the case of HQDS oxidation, the successive-approximation calculations were nonconvergent and the k_b value for that reaction was excluded from the Marcus analysis. For the other reactions, f values ranged from 0.011 to 0.11, and these were used to construct the plots of $\log k_b/f^{1/2}$ versus $\log K_b$. The slope of the least-squares line through the data is 0.42 ± 0.15, in approximate agreement with eq 28. The intercept of the line yields a k_{22} value (pyrazolidone anion/radical self-exchange) of 8×10^5 M^{-1} s^{-1}, the same number afforded by the Marcus analysis of k_c. It is noteworthy that Figure 6 supports the assumption that HQS^-/HSQ and QX^2/SQ^- pairs have self-exchange rate constants (k_{11}) that are very similar. Also, the Marcus analysis suggests that the self-exchange rate constants for **1•**/**1^-** and **2•**/**2^-** are nearly identical since the rate constant for oxidation of hydroquinone by **1•** falls on the same correlation lines as the rate constants for the reactions of **2•**.

It has been observed that rate constants for electron exchange between organic radicals and their parent molecules fall near a value of 10^8 M^{-1} s^{-1} for a variety of systems.[20] Hydroquinone/semiquinone systems appear to be normal in this regard. In terms of Marcus theory, these very rapid electron-exchange reactions are believed to require virtually no internal reorganization of bond lengths and angles; only solvent reorganization is required.[20] One interpretation of "slow" electron exchange between radical and parent is that significant internal-reorganization energy is required during the electron-exchange process. Large internal reorganization has been cited, for example, as the reason for unusually slow self-exchange reactions ($<10^4$ M^{-1} s^{-1}) between tetraalkylhydrazines and their cation radicals.[21,22] Tetraalkyl-hydrazines are approximately pyramidal at each nitrogen, whereas the radical cations are considerably flatter at nitrogen.[21] Evidence that large internal reorganization accompanies the oxidation of

(17) Khan, H. M. T.; Martell, A. E. *J. Am. Chem. Soc.* **1967**, *89*, 4176.
(18) Marcus, R. A. *J. Phys. Chem.* **1963**, *67*, 853.
(19) McCartney, D. H.; McAuley, A. *J. Chem. Soc., Dalton. Trans.* **1984**, 103.

(20) Meisel, D. *Chem. Phys. Lett.* **1975**, *34*, 263.
(21) Nelsen, S. F.; Hintz, P. J.; Buschek, J. M.; Weisman, G. R. *J. Am. Chem. Soc.* **1975**, *97*, 4933.
(22) Nelsen, S. F.; Blackstock, S. C. *J. Am. Chem. Soc.* **1985**, *107*, 7189.

acylated hydrazines has been provided by comparison of vertical ionization potentials with formal redox potentials for several compounds,[23] including 1,2-dimethyl-3-pyrazolidone, which is structurally similar to **1** and **2**. By analogy, perhaps some degree of internal reorganization is required in the electron exchange between a pyrazolidone anion and its radical, and this accounts for the fact that k_{22} is approximately 100 times smaller than k_{11} and other one-electron self-exchange rate constants for "normal" organic systems. Unfortunately, there is insufficient structural detail available for anion and radical to make a valid argument that such reorganization should be expected. Results of semi-empirical calculations (AM1), however, do indicate that the ge-

ometry at the anilino nitrogen in 1-phenyl-3-pyrazolidone (R^1 = R^2 = R^3 = H) is nearly flat, while the corresponding geometry in the anion is more pyramidal. The calculated average bond angle around the anilino nitrogen is 119.7° in the radical and 114.5° in the anion. For tetraalkylhydrazines the geometrical differences between the parent and radical are even greater[21,22] and the electron self-exchange process is correspondingly slower.

Supplementary Material Available: A listing of all pseudo-first-order rate constants determined at varying reactant concentrations, sulfite concentrations, and pH (4 pages). Ordering information is given on any current masthead page.

(23) Nelsen, S. F.; Blackstock, S. C.; Petillo, P. A.; Agmon, I.; Menahem, K. *J. Am. Chem. Soc.* **1987,** *109,* 5724.

Determination of the Enthalpy and Reaction Volume Changes of Organic Photoreactions Using Photoacoustic Calorimetry

Michael S. Herman and Joshua L. Goodman*

Contribution from the Department of Chemistry, University of Rochester, Rochester, New York 14627. Received August 1, 1988

Abstract: Photoacoustic calorimetry (PAC) can be used to measure both the thermal and reaction volume changes for photoinitiated reactions. The photoreactions of 2,3-diazabicyclo[2.2.1]hept-2-ene (DBH), diphenylcyclopropenone (DPC), and *trans*-stilbene (TS) are investigated by PAC. The resolution of these experimental volume changes is accomplished by either a temperature dependence or a binary solvent mixture method. The thermal volume changes yield the enthalpies of reaction in solution, which can be compared to literature values. In two cases (DPH and DPC), the values are more endothermic than those predicted from gas-phase heats of formation. The differences can possibly be attributed to differential solvation of the reactants and products in the polar solvents employed. Absolute reaction volume changes for the photoreactions are also obtained for the photoreactions. PAC is a useful alternative technique to pressure-dependence studies to obtain this information. These volume changes can further be time-resolved to provide kinetic information about the photoprocesses.

The effect of pressure on chemical equilibria and reaction rates has received much attention over the past two decades.[1,2] Attention has been primarily concerned with thermal reactions. Recently, reports have appeared which describe the influence of pressure on photophysical rate constants and the empirical derivation of activation volumes.[3,4] Unfortunately, little information on the reaction volumes of photochemical processes is available. This is due in part to the difficulty in measuring the requisite effect of pressure on the equilibrium constant in photochemical reactions. In selected cases, indirect methods have been used. For example, the reaction volumes of excimer and exciplex formation have been determined by fluorescence intensity measurements.[5] However,

these methods are usually quite restrictive in their application to photochemical systems. Data can be obtained from partial molar volume data or by means of dilatometry, but only when both the reactants and products are stable and isolable. Consequently, it would be quite useful to develop a general methodology to measure photochemical reaction volume changes which involve reactive intermediates.

In this context, we report the use of time-resolved photoacoustic calorimetry (PAC) as an alternative approach to measure reaction volumes of photochemical processes.[6] PAC is extremely sensitive to the volume changes of a chemical system following photoexcitation. These volume changes are caused by both the thermal deposition of energy and the photoinitiated reaction volume change. This paper describes two methods by which these two contributions can be separated and analyzed to provide both enthalpic *and* reaction volume information about the photochemical reaction. In particular, three compounds, 2,3-diazabicyclo[2.2.1]hept-2-ene (DBH), diphenylcyclopropenone (DPC), and *trans*-stilbene (TS), are examined by PAC to illustrate these methods and demonstrate the importance of reaction volume changes in the photoacoustic experiment.

Background

The principles of the photoacoustic effect have been well established.[7,8] When a molecule absorbs a photon, the energy may

(1) (a) Asano, T.; le Noble, W. *Chem. Rev.* **1978,** *78,* 407. (b) le Noble, W. J. *Prog. Phys. Org. Chem.* **1967,** *5,* 207. (c) le Noble, W. *Angew. Chem., Int. Ed. Engl.* **1980,** *19,* 841.

(2) (a) Kelm, H. *High Pressure Chemistry*; Reidel: Boston, 1978; NATO Series. (b) Issacs, N. S. *Liquid Phase High Pressure Chemistry*; Wiley: New York, 1981.

(3) (a) Drickamer, H. G. *Ann. Rev. Phys. Chem.* **1982,** *33,* 25. (b) Offen, H. W. *Organic Molecular Photophysics*; Birks, J. B., Ed.; Wiley: New York, 1973; Vol. 1, p 103.

(4) (a) Turro, N. J.; Okamoto, M.; Gould, I. R.; Moss, R. A.; Lawrynowicz, W.; Hadel, L. M. *J. Am. Chem. Soc.* **1987,** *109,* 4793. (b) Neuman, R. C., Jr.; Berge, C. T. *Tetrahedron Lett.* **1978,** *20,* 1709. (c) le Noble, W. J.; Tamura, K. *Tetrahedron Lett.* **1977,** *19,* 495. (d) Okamoto, M.; Tamura, K. *J. Am. Chem. Soc.* **1986,** *108,* 6378. (e) Hamann, S. D.; Linton, M.; Sasse, W. H. F. *Aust. J. Chem.* **1980,** *33,* 1419.

(5) (a) Braun, v. H.; Forster, T. *Ber. Bunsenges. Phys. Chem.* **1966,** *70,* 1091. (b) Pollmann, P.; Rehm, D.; Weller, A. *Ber. Bunsenges. Phys. Chem.* **1975,** *79,* 692. (c) Pollmann, P.; Weller, A. *Ber. Bunsenges. Phys. Chem.* **1973,** *77,* 692. (d) Seidel, H. P.; Selinger, *Aust. J. Chem.* **1965,** *18,* 977.

(6) (a) Rudzki, J. E.; Goodman, J. L.; Peters, K. S. *J. Am. Chem. Soc.* **1985,** *107,* 7849. (b) Westrick, J. A.; Goodman, J. L.; Peters, K. S. *Biochemistry* **1987,** *26,* 8313.